ACS OMEGA

http://pubs.acs.org/journal/acsodf

Article

Triple Silicon, Phosphorous, and Nitrogen-Grafted Lignin-Based Flame Retardant and Its Vulcanization Promotion for Styrene Butadiene Rubber

Jianxing Li, Zepei Yan, Ming Liu, Xiaokun Han, Tianyun Lu, Ruiyin Liu, Shugao Zhao, Qing Lv, Bo Li, Shengqin Zhao,* and He Wang*

Cite This: *ACS Omega* 2023, 8, 21549−21558

Read Online

ACCESS | Metrics & More | Article Recommendations

ABSTRACT: In this study, we present an innovative environmental silicon-, phosphorus-, and nitrogen-triple lignin-based flame retardant (Lig-K-DOPO). Lig-K-DOPO was successfully prepared by condensation of lignin with flame retardant intermediate DOPO-KH550 synthesized via Atherton−Todd reaction between 9, 10-dihydro-9-oxa-10-phosphaphenanthrene-10-oxide (DOPO) and γ-aminopropyl triethoxysilane (KH550A). The presence of silicon, phosphate, and nitrogen groups was characterized by FTIR, XPS, and ^{31}P NMR spectroscopy. Lig-K-DOPO exhibited advanced thermal stability compared with pristine lignin supported by TGA analysis. The curing characteristic measurement showed that addition of Lig-K-DOPO promoted the curing rate and crosslink density to styrene butadiene rubber (SBR). Moreover, the cone calorimetry results indicated Lig-K-DOPO conferred impressive flame retardancy and smoke suppression. The addition of 20 phr Lig-K-DOPO reduced SBR blends 19.1% peak heat release rate (PHRR), 13.2% total heat release (THR), 53.2% smoke production rate (SPR), and 45.7% peak smoke production rate (PSPR). This strategy provides insights into multifunctional additives and greatly extends the comprehensive utilization of industrial lignin.

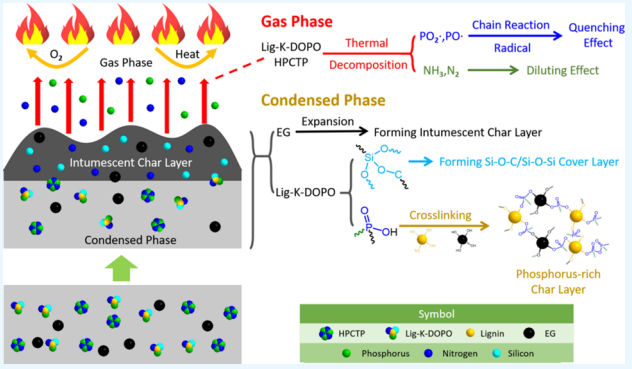

1. INTRODUCTION

In recent years, polymer materials are widely used for various applications but mostly exhibit disadvantages such as poor fire retardancy and thermal stability, which limit their applications in specific fields where high levels of fire safety are required. Therefore, the addition of flame retardants plays a key role in the enhancement of flame retardancy properties of polymer materials. Considering environmental protection and human health, an increasing number of countries have promulgated bans on halogen-containing flame retardants.[1] Halogen-free flame retardants such as P-, N-, and Si-containing flame retardants and metallic hydroxides have been considered alternatives to halogen-containing flame retardants owing to their reduced environmental impact and high efficiency.[2] However, research indicates that synergy between a single P−N compound flame-retardant system and a synergist is usually required for a high flame-retardant performance.[3] Xu et al. evaluated a phosphorous-based bi-functional compound HPDAl that was used as a reactive-type flame retardant (FR) in an epoxy thermoset (EP) aiming to improve the flame retardant efficiency of phosphorus-based compounds.[4] Their results showed that adding 2 wt % HPDAl made EP composites acquire an LOI value of 32.3%, pass a UL94 V-0 rating with a blowing-out effect, and exhibit a decrease in the heat/smoke release. Kong et al. evaluated the efficiency of organic montmorillonite intercalation cobalt hydroxides modified by acidified chitosan (Co-OMt) as a synergistic agent in an intumescent polypropylene (PP) system based on ammonium polyphosphate (APP) and pentaerythritol (PER).[5] Their results showed that layered Co-OMt was not only uniformly dispersed in the PP matrix but also accelerated the advancement of the intumescent shield which can effectively isolate heat conduct between the flame and substrate. Although the layered Co-OMt exhibited excellent flame resistance, the environmental hazard of cobalt compounds cannot be neglected. Wang et al. adopted nitrogenous bases as a bio-based gas to synergize with IFR.[6] They concluded that the formation of cellular and intumescent char layers could be

Received: February 3, 2023
Accepted: May 24, 2023
Published: June 5, 2023

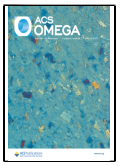

https://doi.org/10.1021/acsomega.3c00714
ACS Omega 2023, 8, 21549−21558

promoted, and the flame retardancy of PP could be improved with the incorporation of uracil (U). This investigation proved that bio-based synergists have comparable efficiency to their current non-bio-based counterparts. As their sustainability and environmental benefits, bio-based synergists/flame retardants hold tremendous benefits.

Lignin is the second most abundant biopolymer from nature which is considered as a sustainable and environmentally friendly material and renewable resource.[7−9] However, approximately 95% of industrial lignin from the paper industry is disposed of as industrial waste, necessitating the comprehensive utilization of industrial lignin. In recent years, the use of lignin in polymer applications has gained interest due to its excellent flame-retarding potential of pristine lignin and its derivatives in a wide range of polymeric materials.[10,11] However, the active sites of the aromatic ring in lignin have a large steric hindrance and low reactivity.[12] Besides, the flame retardancy effect of pristine lignin is usually limited. To improve the flame retardancy efficiency of lignin, functionalization or synergistic combination with other effective flame retardants to maximize the use of the char-forming property of lignin has drawn considerable attention.[13,14] Liu et al. successfully modified lignin with N and P (F-lignin) via a catalytic effect of Cu^{2+}, and the continuous and intact char layer of F-Lignin contributed to the improvement to the flame retardancy of PP.[15] However, the thermal stability of F-Lignin declined slightly which restricts the further enhancement of its flame retardancy compared to the origin lignin (O-lignin). In order to intensify the flame resistance of lignin, Zhou et al. fabricated an N/P-modified lignin-based flame retardant by a mild two-step method which resulted in lower char-forming temperature, enhanced thermal stability, and char formation in epoxy resin (EP).[16] Howbeit, the addition of modified lignin showed a negative impact on the intensive deterioration of EP's mechanical properties. Zhu et al. chemically grafted lignin with N/P-containing groups via a liquefaction-esterification-salification process to prepare a lignin-based phosphate melamine compound (LPMC), which was then used to modify polyurethane (PU), thereby improving the flame retardancy of PU.[17] This work inspired the research on multifunctional lignin-based additives. However, smoke suppression among the most important evaluations of flame retardants has lacked interest in this research. To the best of our knowledge, there are still some challenges in improving lignin-based flame retardant: (i) the increment of thermal properties, which can be realized by the introduction of silicon,[18] (ii) the development of fire resistance efficiency, especially the escalation of smoke suppression, which can be achieved by the synergistic effect of phosphorus, nitrogen, and silicon,[19] and (iii) the impairment of matrix mechanical properties due to lignin aggregation, which can be mitigated by decrement of lignin surface polarity.[20]

Styrene butadiene rubber (SBR), a commonly used synthetic rubber, is highly inflammable, which restricts its use for flame retardancy applications.[21] However, with the emergence of novel efficient halogen-free flame retardants such as ammonium polyphosphate,[22,23] SBR is commonly used in various applications, such as in conveyor belts in the coal mining industry[24] and decorative materials like carpets.[22]

The thermal stability of lignin which was modified by Liu et al. declined slightly.[15] Zhou et al. fabricated a lignin-based flame retardant that enhanced the thermal stability by a mild two-step method resulted.[16] However, the addition of the modified lignin had a negative effect on the mechanical properties of the matrix. In this study, a novel N-, P-, and Si-type lignin-based flame-retardant, Lig-K-DOPO, was prepared according to the Atherton−Todd reaction and then coordinated with hexaphenoxy cyclophosphazene (HPCTP)/expandable graphite (EG) to enhance the flame retardancy of SBR composites while reducing the effect of lignin on the mechanical properties. The chemical structure and thermal stability of Lig-K-DOPO were characterized by using Fourier-transform infrared (FTIR) spectroscopy, X-ray photoelectron spectroscopy (XPS), and ^{31}P nuclear magnetic resonance (^{31}P NMR). The effects of the modified Lig-K-DOPO on the curing characteristics, crosslinking density, filler dispersion, and physical-mechanical and flame-retardant properties of the SBR composites were fully investigated and compared to those of pristine lignin. The flame-retardant mechanism of this novel functionalized lignin in SBR composites is also discussed.

2. EXPERIMENTAL SECTION

2.1. Materials. SBR 1502 was provided by Shandong Qilu Petrochemical Engineering Co., Ltd., China. Lignin was purchased from Shandong Longlive Biotechnology Co., Ltd., China. Highly dispersible amorphous silica precipitate (grade Zeosil 1165MP) was manufactured by Rhodia Silica Co., Ltd., Qingdao, Shandong Province, China. 3-Aminopropyltriethoxysilane (KH550) and 9,10-dihydro-9-oxa-10-phosphaphenanthrene-10-oxide (DOPO) were purchased from Shanghai Aladdin Biochemical Technology Co., Ltd., China. HPCTP was provided by Shandong Taixing New Material Co., Ltd., China. EG was supplied by Qingdao Tianheda Graphite Co., Ltd., China. Triethylamine ($C_6H_{15}N$/TEA/Et_3N), carbon tetrachloride (CCl_4), dichloromethane (CH_2Cl_2), and ethanol (C_2H_5OH) were analytical-grade products and used as received. All rubber additives, such as sulfur (S), stearic acid (SA), zinc oxide (ZnO), the antioxidant N-(1,3-dimethylbutyl)-*N*′-phenyl-*p*-phenylenediamine (4020), the accelerator N-tert-butyl-2-benzothiazole sulfonamide (TBBS), 2,2′-dithiodibenzothiazole (DM), the anti-scorch agent N-cyclohexylthiophthalimide (CTP), and the silane coupling agent bis-(3-triethoxysilylpropyl) tetrasulfide (Si69), were industrial-grade products and used as received.

2.2. Synthesis of Lig-K-DOPO. DOPO-KH550 was synthesized by the Atherton−Todd reaction as an intermediate for the preparation of Lig-K-DOPO. First, 100 g of the flame-retardant intermediate, DOPO, was dissolved in 100 mL of CH_2Cl_2. Subsequently, 100 g of KH550 and 50 g of Et_3N were slowly added to the mixture under continuous magnetic stirring in a nitrogen atmosphere. The mixture was cooled below 20 °C in an ice bath and stirred continuously until DOPO was completely dissolved. Thereafter, 400 g of CCl_4 was slowly added dropwise over 60 min to ensure that the temperature did not exceed 20 °C. After the addition of CCl_4, the system was heated to 23 °C and stirred for 12 h. The mixture was then filtered and rinsed with water at least three times. Finally, the flushed product was dried under vacuum at 70 °C for 36 h to obtain a yellowish product.

The graft reaction between DOPO-KH550 and lignin was initiated by silanization. For the reaction, 60 g of lignin and DOPO-KH550 and 800 mL of C_2H_5OH were added to a three-necked round-bottom flask equipped with a nitrogen inlet and condenser. The mixture was then heated to 70 °C and stirred for 12 h. After completion of the reaction, the as-obtained product was centrifuged, washed, and vacuum-dried

https://doi.org/10.1021/acsomega.3c00714
ACS Omega 2023, 8, 21549−21558

Scheme 1. Synthesis Route of Lig-K-DOPO

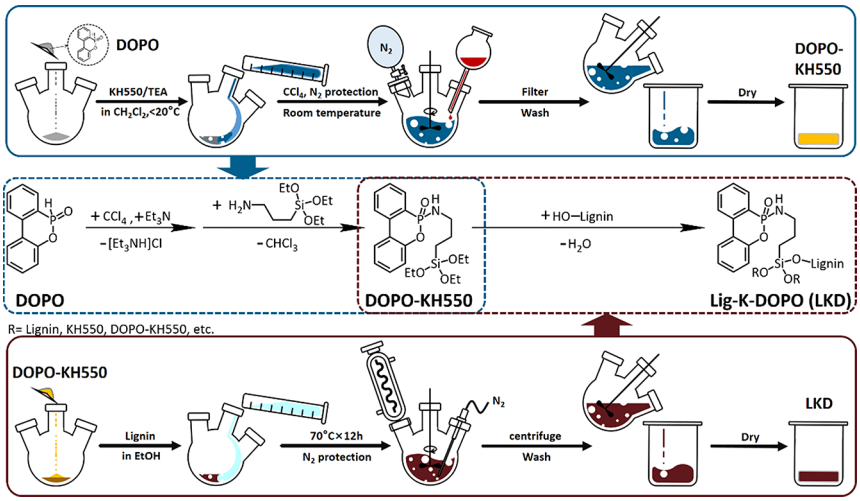

to obtain a brown product. The synthesis of Lig-K-DOPO is illustrated in Scheme 1.

Both, lignin and the prepared Lig-K-DOPO, were processed by ball milling to reduce the size of the lignin/Lig-K-DOPO particles.

2.3. Synthesis of Composites with SBR. The experimental formulations of all the SBR composites are listed in Table 1. First, SBR gum, silica, Si69, and lignin/Lig-K-DOPO were mixed in an internal mixer at a fill factor of 0.7 at 80 °C. Next, the composites were mixed for 5 min till the mixing temperature reached 140 °C to ensure that the silylation reaction of the composites was completed. Subsequently, the obtained material was cooled to room temperature.

Table 1. Formulation of SBR Composites[a]

	samples			
ingredients [phr]	SBR	SBR/20 Lig	SBR/10 LKD	SBR/20 LKD
SBR	100	100	100	100
Lig-K-DOPO	0	0	10	20
lignin	0	20	0	0

[a]All weights are in parts per 100 g of rubber (phr): silica 50, HPCTP 30, EG 20, ZnO 5, stearic acid 2, antioxidant 4020 3, accelerator NS 1.5, accelerator DM 1, sulfur 1.5, CTP 0.3, and Si69 4 were common to all the mixtures.

Second, the as-prepared composites and rubber additives other than sulfur were mixed in an internal mixer at 60 °C at a rotor speed of 60 r·min^{-1}. Sulfur was then added to a laboratory-size two-roll mill (Φ160 × 320) to obtain 2 mm-thick sheets. Subsequently, the rubber compounds were press-cured at 160 °C for an optimum curing time of 2 min.

The experiment used SBR and SBR with 20 phr lignin dual-control, marked as SBR and SBR/20 Lig, respectively. SBR/10 LKD and SBR/20 LKD were SBR/HPCTP/EG composites with 10 and 20 phr of the flame-retardant Lig-K-DOPO, respectively.

2.4. Characterizations. *2.4.1. Fourier-Transform Infrared Spectroscopy.* FTIR spectra were recorded in the attenuated total reflection mode with a Vertex 70 FTIR spectrometer (Bruker, Germany), and the wavenumber range was set to 500−4000 cm^{-1}.

2.4.2. Nuclear Magnetic Resonance (NMR) Spectroscopy. ^{31}P NMR spectra were recorded on a Bruker AVANCE-500 MHz NMR spectrometer at 300 K using dimethyl sulfoxide (DMSO-d6) as the solvent.

2.4.3. X-ray Photoelectron Spectroscopy (XPS). The changes in the functional groups on the modified lignin particle surfaces were examined by XPS using a Thermo ESCALAB Xi+ instrument with a monochromatized Al Kα radiation source (200 W). The acquired XPS profiles identified peaks for the C 1s, O 1s, N 1s, Si 2p, and P 2p orbitals.

2.4.4. Thermal Stability. Thermogravimetric analysis (TGA) was performed using a TG 209 F1 thermogravimetric analyzer (NETZSCH, Germany). The lignin and Lig-K-DOPO powders were heated from 30 to 700 °C at a heating rate of 20 K·min^{-1} under a nitrogen atmosphere.

2.4.5. Curing Characteristic. A moving-die rheometer MDR 2000 was used to determine the curing characteristics of the compounds at 170 °C, 1.67 Hz frequency, and 7% strain. The torque vs time curves were recorded, and curing parameters such as the maximum torque (M_H), minimum torque (M_L), difference in torque (M_H−M_L), scorch time (t_{10}), and optimum curing time (t_{90}) were determined. The curing rate index (CRI) was calculated using eq 1.

$$\mathrm{CRI} = 100/(t_{90} - t_{10}) \tag{1}$$

2.4.6. Crosslink Density Measurement. The vulcanizates were immersed in toluene for 72 h at room temperature to reach the equilibrium swelling state. The swollen sample was then dried in a vacuum oven to reach a constant weight for 36 h at 60 °C. The weights of the vulcanizate samples before swelling (m_0), after swelling (m_1), and vacuum-drying (m_2) were measured. The crosslinking density (V_e, mol·cm^{-3}) according to the Flory−Rehner equation and the rubber volume fraction (V_r) in the swollen sample are expressed in eqs 2 and 3), respectively,

$$V_e = -\frac{\ln(1 - V_r) + V_r + \chi V_r^2}{V_s \cdot (V_r^{1/3} - V_r/2)} \tag{2}$$

$$V_r = \frac{m_0 \times \varphi \times (1 - \alpha)/\rho_r}{m_0 \times \varphi \times \frac{(1-\alpha)}{\rho_r} + \frac{(m_1 - m_2)}{\rho_s}} \tag{3}$$

https://doi.org/10.1021/acsomega.3c00714
ACS Omega 2023, 8, 21549−21558

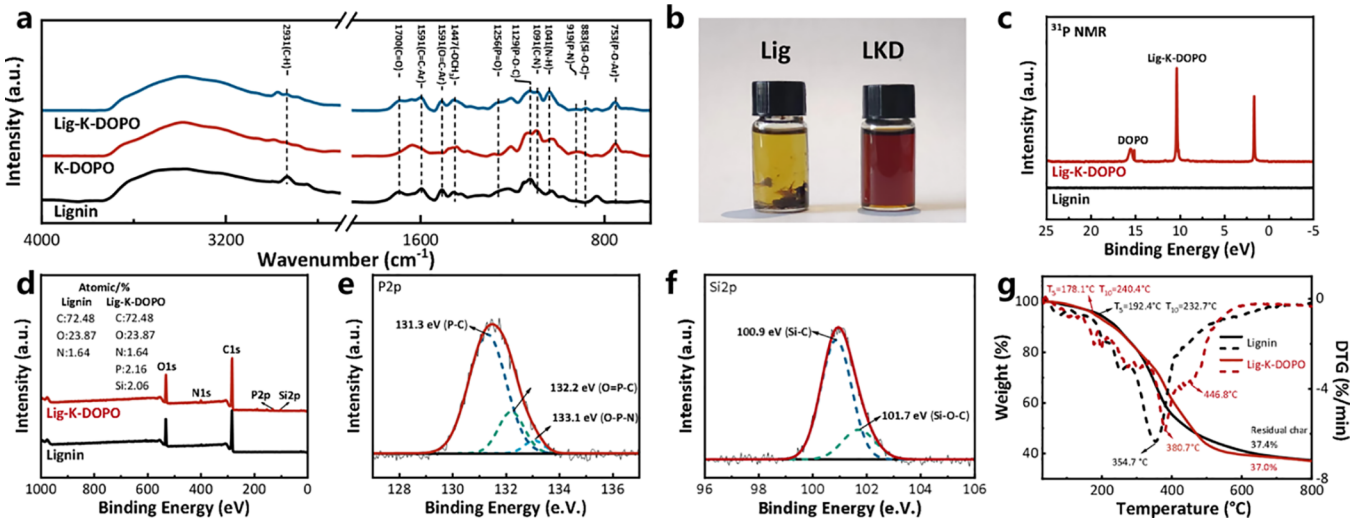

Figure 1. FTIR spectra of lignin, DOPO-KH550, and Lig-K-DOPO (a); dissolved characteristics of lignin and Lig-K-DOPO in DMSO (b); ^{31}P NMR XPS spectra of lignin and Lig-K-DOPO (c); XPS element analysis of lignin and Lig-K-DOPO (d); XPS P 2p spectrum analysis of Lig-K-DOPO (e); XPS Si2p spectrum analysis of Lig-K-DOPO (f); TGA of lignin and Lig-K-DOPO (g).

where φ is the proportion of rubber in the composite, α is the proportion of mass loss during swelling, ρ_r is the density of the rubber (g·cm^{-3}), ρ_s is the density of the solvent (g·cm^{-3}), V_s is the molar volume of toluene (106.28 cm^3·mol^{-1}), and χ is the rubber−solvent interaction parameter. The χ between SBR and toluene is 0.446.[25]

2.4.7. RPA Analysis. The rubber process analyzer RPA 2000 was used to measure the strain dependence of the elastic modulus and loss factor of the uncured samples in the strain range of 0.28−200% at 60 °C and a frequency of 1 Hz.

2.4.8. Physical Mechanical Properties. The hardness was measured with reference to the ASTM D-2240 standard. The tensile properties were determined using a Zwick BT1-FR005TN A50 tensile tester using dumbbell-shaped specimens with a crosshead speed of 500 mm·min^{-1} with reference to the ASTM D-412 standard. All the tests were performed at 25 ± 2 °C.

2.4.9. Scanning Electron Microscopy. The fractured surfaces of the SBR vulcanizates were observed using scanning electron microscopy (SEM, JEOL JSM-7500F, Japan). The specimens were coated with a conductive gold layer.

2.4.10. Flame Property Test. The LOI was measured using an HC-2 oxygen index analyzer (Nanjing Jiangning Analytical Instrument Co., Ltd., China) with reference to the ASTM D-2863 standard. The dimensions of the specimens were 120 × 6.5 × 3 mm^3.

The fire performance was evaluated using a CONE 6810 cone calorimeter (Vouch Testing Technology Co., Ltd.) according to ISO 5660 standard procedures. Square specimens (100 × 100 × 4 mm^3) wrapped in aluminum foil were placed on a holder and irradiated at a heat flux of 50 kW·m^{-2}.

3. RESULTS AND DISCUSSION

3.1. Characterization of Lig-K-DOPO. To characterize the chemical structure of Lig-K-DOPO, the FTIR and XPS profiles of lignin and Lig-K-DOPO are shown in Figure 1a. We observed that the stretching vibration bonds of C−H on the aliphatic molecular chain (2931 cm^{-1}), C═O without conjugation with the benzene ring (1700 cm^{-1}), C═C of the lignin aromatic skeleton (1591 cm^{-1}), C═O with aromatic nature (1504 cm^{-1}),[26] and −OCH3 (1447 cm^{-1}) appear in the FTIR spectrum of lignin.[27] Compared to lignin, the new absorption peak observed at 753 cm^{-1} belongs to the stretching vibration of the P−O−Ph bond stemming from DOPO. The peaks at 1129 and 1256 cm^{-1}, which are associated with the P−O−C and P═O bonds, respectively, are observed for Lig-K-DOPO. Moreover, the absorption peak at 1091 cm^{-1} correlates to the presence of C−N bonds in the KH550 structure. These findings suggest that lignin is graft-modified by P and N. In addition, the characteristic absorption peaks at 919 and 1041 cm^{-1} are related to the stretching vibrations of the C−N and N−H bonds, which could be generated by the Atherton−Todd reaction of DOPO and KH550. The appearance of the absorption peak at 883 cm^{-1} is ascribed to the vibration absorption of the Si−O−C bond, indicating that dehydration condensation occurs between the hydroxyl group of lignin and the silanol of KH550. A clear dispersion of lignin and Lig-K-DOPO in DMSO can be observed in Figure 1b.

^{31}P NMR was performed to further reveal the elemental states and chemical structure of Lig-K-DOPO. In the ^{31}P NMR spectra depicted in Figure 1c, the signal at 15.54 ppm is attributed to the P of phosphaphenanthrene in DOPO,[28] and the peak at 10.35 ppm is due to the P in Lig-K-DOPO.[29] Besides, the peak at 1.7 ppm is presumed to arise from the formation of a DOPO-based phosphonate ammonium salt byproduct.[30]

XPS was performed to obtain information about the elemental composition and content of lignin and Lig-K-DOPO, and the results are shown in Figure 1d. The XPS profile of lignin only shows the presence of C, O, and a small amount of N. In contrast, the XPS survey spectrum of Lig-K-DOPO clearly shows the existence of P, Si, and excess N, apart from C and O, confirming the successful decoration of lignin with DOPO via the linkages of KH550. The substituent bound to the atom of concern leads to shifts in the binding energy of this atom, as revealed by the XPS profiles. Therefore, functional groups possess a specialized shift, the binding energy of which can be found in the literature. Considering the variety of structures of C and O in lignin, and the N that emerges during lignin production, only the XPS P 2p and Si 2p spectra were used to analyze the structural differences between

https://doi.org/10.1021/acsomega.3c00714
ACS Omega 2023, 8, 21549−21558

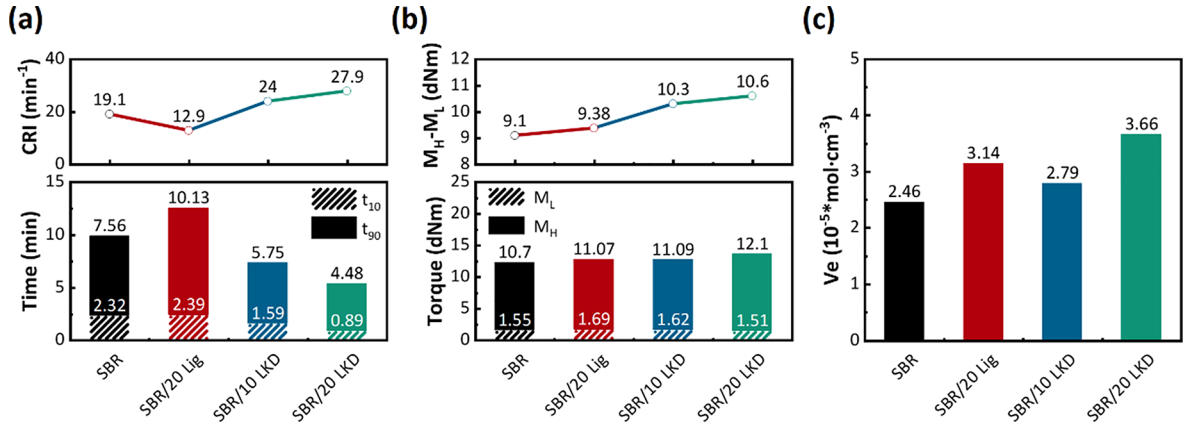

Figure 2. t_{10}, t_{90}, and CRI of composites (a); M_L, M_H, and M_H-M_L of composites (b); crosslink density of composites (c).

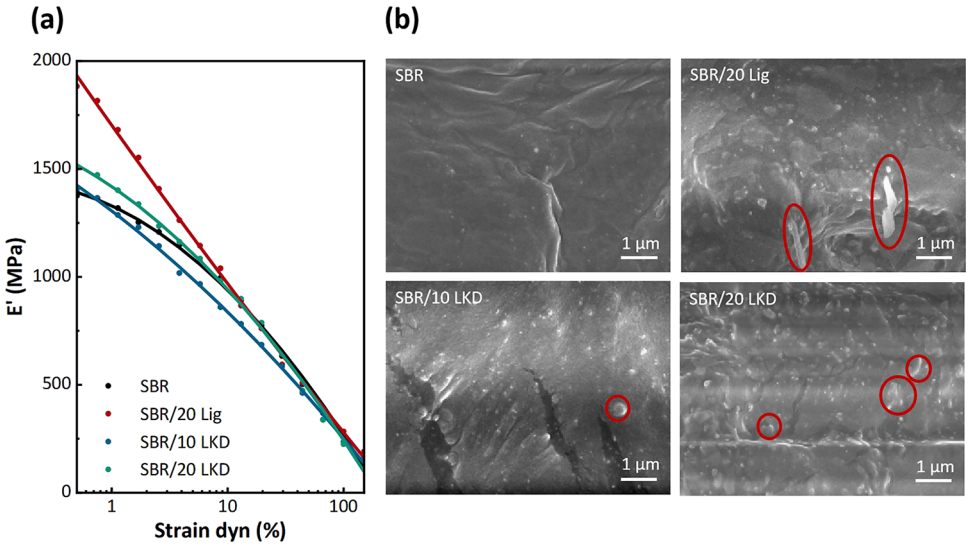

Figure 3. Effect of Lig-K-DOPO on dynamic mechanical properties of SBR compounds (a); SEM micrographs of lignin/Lig-K-DOPO-filled SBR vulcanizates (b).

lignin and Lig-K-DOPO, and the results are presented in Figure 1e,f. The P 2p XPS profile is deconvoluted into three components: P−C bonds at 131.3 eV, the O═P−C bond at 132.2 eV, and the O−P−N bond at 133.1 eV. The existence of the O−P−N bond implies the occurrence of a reaction between the P−H and $-NH_2$ bonds in DOPO and KH550, respectively. The high-resolution Si 2p band of Lig-K-DOPO is split into two peaks corresponding to Si−C (100.9 eV) and Si−O−C (101.7 eV) bonds, respectively. The presence of Si−O−C can indicate dehydration condensation between lignin and KH550. This indicates that DOPO reacts with lignin via KH550. Therefore, it can be concluded that DOPO was chemically grafted onto the lignin surface via linkages with KH550.

To compare the thermal stability of lignin and Lig-K-DOPO, the thermogravimetric and derivative thermogravimetric (DTG) curves are presented in Figure 1g. The lignin decomposes in several steps up to 800 °C.[31−33] Lignin starts to decompose (the initial decomposition temperature at 5% weight loss, T5) at approximately 192.4 °C and exhibits a maximum weight loss temperature (T_{max}) of 354.7 °C. In the range of 30−280 °C, the water loss and decomposition of ether linkages[29] and side branches occur. Subsequently, in the main degradation step (280−500 °C),[34] the scission of C−C and $\beta-\beta$ linkages leads to the creation of CH_4 and cleavage of the main lignin chain,[35] Above 500 °C, char formation occurs owing to further rearrangement and condensation of the aromatic structure.[36]

After lignin was modified by KH550 and DOPO, Lig-K-DOPO exhibited a lower T_{onset} than lignin. However, Lig-K-DOPO exhibited two relatively higher T_{max} values, which indicated that the decomposition process of the modified lignin was substantially altered by incorporating P, N, and Si. The much higher T_{max} of Lig-K-DOPO was beneficial for protecting the much higher char residue produced at a relatively low temperature. The char residue at 800 °C and 37.0 wt % for Lig-K-DOPO was similar to that of lignin, indicating that both, lignin and Lig-K-DOPO, can be used as excellent char-forming agents. Char formation at high temperatures would be beneficial to insulate heat and mass transfer, block oxygen, and decrease the rate of combustion of the polymer.

3.2. Cure Characteristics of SBR Composites. The curing parameters of the sulfur-cured SBR compounds are summarized in Figure 2. Compared to SBR, the addition of pristine lignin prolongs the t_{10} and t_{90} of SBR/20 Lig and decreases the CRI. This is because polar lignin can interact

https://doi.org/10.1021/acsomega.3c00714
ACS Omega 2023, 8, 21549−21558

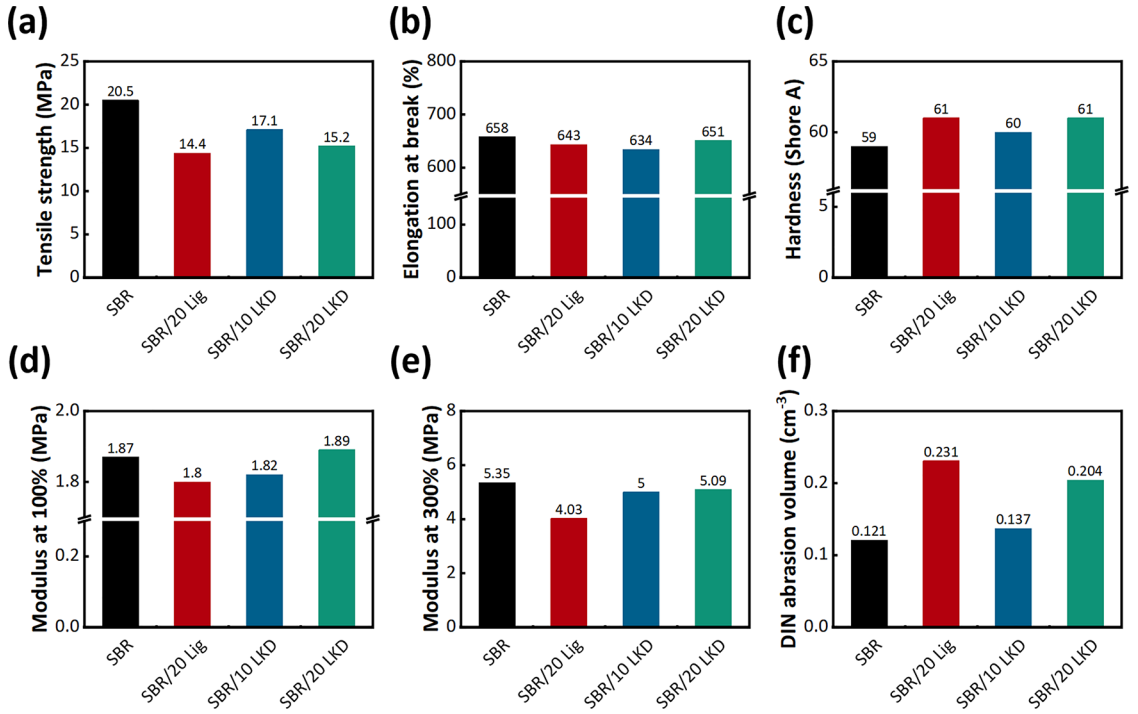

Figure 4. Mechanical properties of SBR vulcanizates tensile strength (a); elongation at break (b); hardness (c); modulus at 100% (d); modulus at 300% (e); DIN abrasion volume (f).

with the curing agents and adsorb the molecules of the accelerator and other curing agents onto its surface.

For Lig-K-DOPO, it is evident that the modification of lignin significantly reduces t_{10} and t_{90}, the $M_H - M_L$ of the SBR compounds slightly increases, and the crosslinking density and CRI increase with increasing concentration of Lig-K-DOPO. Thus, the modification of lignin contributed to the following two effects. The adsorption of curing agents on Lig-K-DOPO could be suppressed owing to the decrease in the number of hydroxyl groups on the surface of Lig-K-DOPO caused by dehydration condensation with KH550. The tertiary amine group of Lig-K-DOPO would be beneficial for activating the curing rate for sulfur-cured SBR compounds.

3.3. Filler Dispersion. Based on strain sweep measurements, the nonlinear viscoelastic nature of the composites, where the shear storage modulus G' decreases sharply with the strain increment, is known as the Payne effect. The Payne effect amplitude is the difference between G' at a low strain and G' at a high strain ($\Delta G'$), and is an indication of the filler−filler interaction. Generally, the higher the Payne effect amplitude, the poorer is the filler dispersion. The dependence of G' on the strain of the SBR composites is shown in Figure 3a. Compared to the control sample of SBR, the SBR/20 Lig compound shows the highest $\Delta G'$, reflecting the poor dispersibility of unmodified lignin in SBR, which is related to the van der Waals forces generated by the polar functional moiety in the lignin structure. When lignin was modified by adding Lig-K-DOPO, better filler dispersion, particularly at a low loading of 10 phr, was observed.

The dispersion of lignin and morphology of the SBR-lignin systems were further investigated using SEM, and the results are presented in Figure 3b. Pristine lignin is poorly dispersed and severely aggregated in the SBR matrix, which is shown as embedded microparticles with clear edges in the SEM image of the SBR/20 Lig composite. This may be attributed to the incompatibility in polarity. When lignin was chemically modified, adding Lig-K-DOPO resulted in better filler dispersion in the SBR/10 LKD and SBR/20 LKD vulcanizates. When the lignin loading was 10 phr, the small lignin particles in the SBR matrix were homogeneously dispersed, which was attributed to the decrease in the number of hydroxyl groups on the surface of lignin and the enhanced interfacial bonding between the lignin and the rubber matrix using a coupling agent.

3.4. Mechanical Properties of SBR Vulcanizates. The mechanical properties of SBR vulcanizates are closely related to the degree of filler dispersion and the crosslinking density. The effects of lignin/Lig-K-DOPO loading on the tensile strength, elongation at break, modulus, hardness, and wear properties are observed from the data plotted in Figure 4. First, the lignin/Lig-K-DOPO loading had no distinct effect on the hardness of SBR vulcanizates. Compared to the control sample of SBR, the tensile strength, modulus at 300% elongation, and abrasion resistance of SBR/20 Lig are significantly reduced. This is attributed to the poor dispersion of lignin in the hydrophobic rubber matrix, which easily leads to stress concentration when the material is subjected to a tensile pull test, which reduces the ultimate strength of the composite. The deterioration of the mechanical properties of SBR/20 LKD can also be attributed to the participation of Lig-K-DOPO. However, unlike lignin, when the dosage of Lig-K-DOPO is 10 phr, SBR/10 LKD exhibits relatively good mechanical properties.[37,38] Nevertheless, all the mechanical properties of SBR/20 LKD are better than those of SBR/20 Lig vulcanizates, indicating better reinforcement of Lig-K-DOPO than the unmodified lignin.

3.5. Flame Properties. A cone calorimeter was used to determine the characteristic combustion parameters correlated with real fire disasters. The heat release rate (HRR), peak HRR (PHRR), and time of arrival at PHRR (tPHRR) are shown in

https://doi.org/10.1021/acsomega.3c00714
ACS Omega 2023, 8, 21549−21558

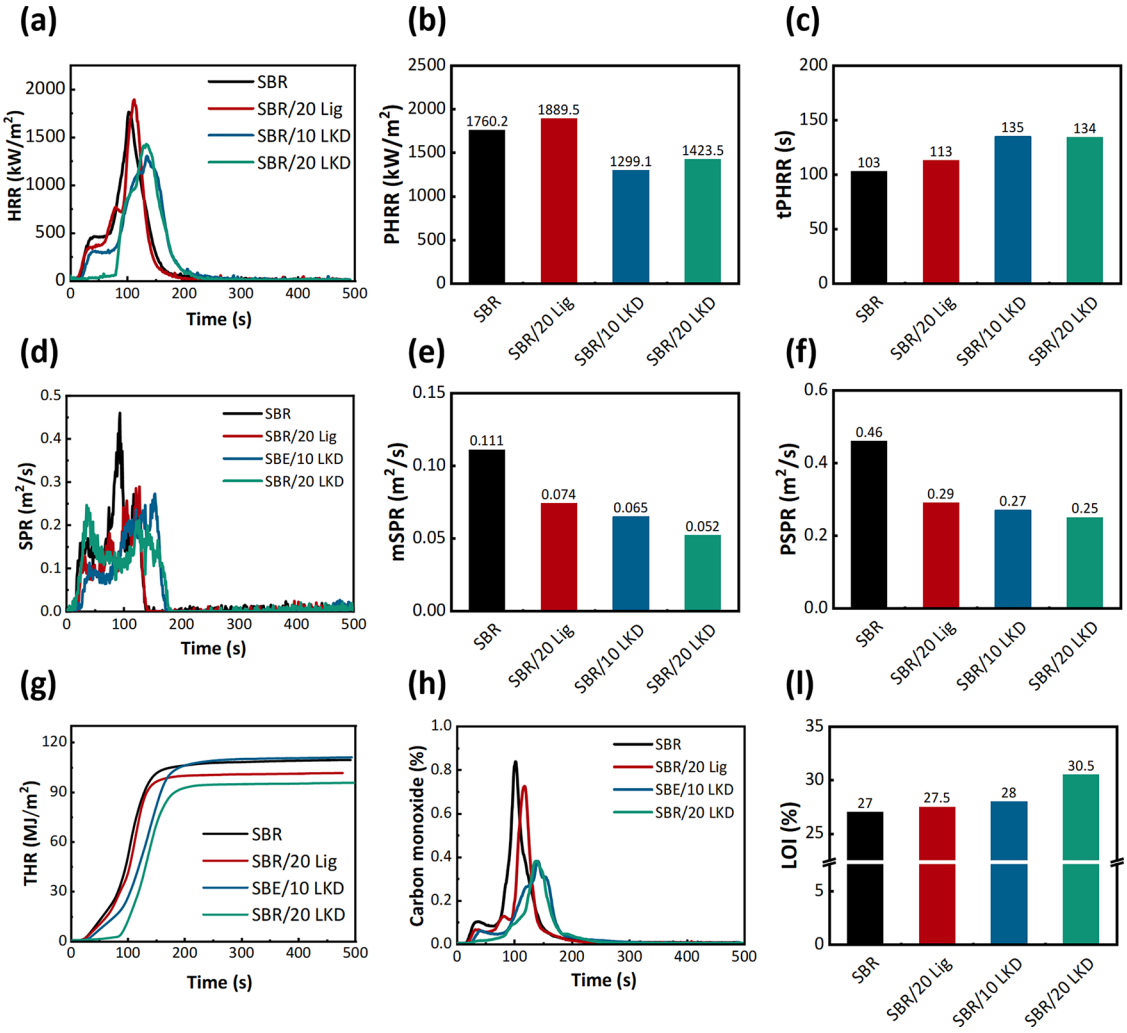

Figure 5. Effect of Lig-K-DOPO on HRRs (a–c), SPRs (d–f), THR (g), carbon monoxide concentration of released gas (h), and LOI (l).

Figure 5a–c. The SBR/20 Lig vulcanizate presents a higher PHRR and a slight prolongation in the tPHRR. The PHRRs of SBR/Lig-K-DOPO vulcanizates are significantly reduced, and the tPHRR values are significantly prolonged. Furthermore, with increasing Lig-K-DOPO, the PHRR of SBR vulcanizates decreases.

The smoke-related parameters are analyzed in Figure 5d–f, including the smoke production rate (SPR), peak smoke production rate (PSPR), and average smoke release rate within 5 min (mSPR). Compared with the SBR, the PSPR and mSPR values are reduced by both, lignin and Lig-K-DOPO, to varying degrees, indicating a reduction in smoke hazards with an increase in Lig-K-DOPO.

The total heat release (THR) of materials is another important flame-retardant parameter for evaluating flame hazards. Typically, a qualified flame-retardant material will exhibit a lower THR, which can effectively inhibit the continuous spread of the flame during combustion. As shown in Figure 5g, SBR/20 Lig exhibits a decreased THR compared to the control sample, which is attributed to the condensation carbonization of aromatic lignin. SBR/20 LKD shows the lowest THR, 95.5 MJ m^{-2}, as an indicator of the synergy of P and N in Lig-K-DOPO. Note that although a low loading of Lig-K-DOPO is beneficial for decreasing the PHRR of SBR vulcanizates, it is not sufficient to decrease the THR.

In a practical fire, the release of poisonous gases, such as carbon monoxide (CO), is also the dominant factor that causes personnel casualties, as shown in Figure 5h. In this regard, the SBR/LKD materials enable a considerable abatement of CO release, which can significantly mitigate the harm caused by the poisonous gas.

The flammability of the SBR composites was further evaluated using LOI analysis (Figure 5i). The LOI of the control SBR sample with the addition of HPCTP and EG is approximately 27%. For the SBR/20 Lig vulcanizate, the addition of lignin slightly improves the LOI. Thus, adding Lig-K-DOPO can effectively improve the LOI of SBR vulcanizates, which further proves the feasibility of attaining an intrinsic flame retardancy in lignin by introducing P, N, and Si into its structure.

3.6. Flame Retardant Mechanism. The flame retardant mechanism of SBR filled with Lig-K-DOPO is mainly attributed to the effects of HPCTP, EG, and Lig-K-DOPO, as illustrated in Scheme 2. The cyclic phosphazene cores of HPCTP decompose into substantial amounts of P-free radicals (PO_2· and PO·), and nonflammable nitrogen pyrolysis gas flows toward the gas phase because of the phosphazene structure in HPCTP. These pyrolytic PO_2· and PO· free radicals react with flammable radicals, such as H· and OH·, to reduce the opportunity for combustion, leading to a quenching

https://doi.org/10.1021/acsomega.3c00714
ACS Omega 2023, 8, 21549−21558

Scheme 2. Flame Retardant Mechanism of SBR/Lig-K-DOPO

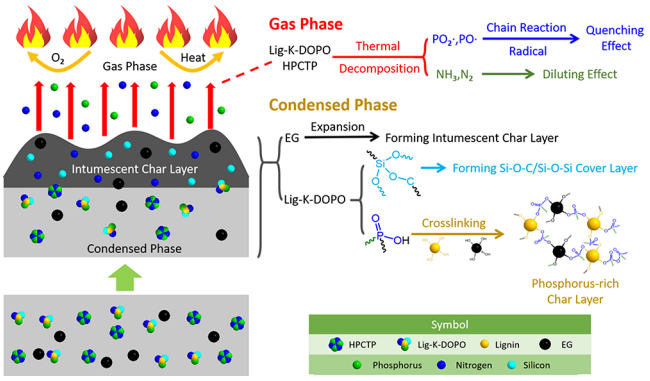

effect. Meanwhile, the nonflammable CO_2, N_2, and NH_3 gases formed from HPCTP decrease the concentration of the flammable gas to produce a diluting effect. In contrast, in the condensed phase, the cyclic phosphazene structure becomes a P-rich pyrolysis fragment and promotes the formation of charring layers. The P-rich fragments with high molecular weights in the char will also improve the thermal stability of the charring layers and prevent further combustion of the interior matrix in the condensed phase. All these reasons, including the quenching and diluting effects of flame inhibition in the gas phase and the charring effect in the condensed phase, confirm the flame-retardant effectiveness derived from the addition of HPCTP.[39] EG was heated to produce expanded graphite flakes and formed a "worm-like" structure due to the "popcorn effect", producing nonflammable gases like CO_2 and forming the char layer.[40] Moreover, char formation accelerated the effect of Lig-K-DOPO in combination with EG, which can further enhance the flame retardancy of the materials.

Lig-K-DOPO exerted a flame-retardant effect in both, condensed and gas phases. In the gas phase, the DOPO group in Lig-K-DOPO can generate P radicals (such as PO· and PO_2) during pyrolysis, such as HPCTP, which can also quench active radicals (such as OH·, H·, and hydrocarbon) to interrupt the free radical chain reaction of combustion and capture active terminal free radicals in the molecular chain of the decomposed matrix to inhibit further degradation of the matrix.[41] Furthermore, the amino group in Lig-K-DOPO may decompose into nonflammable gases such as NH_3 and N_2. These nonflammable nitrogenous gases can dilute ignitable gases, cut off the oxygen supply, and remove heat during combustion. In the condensed phase, the thermal degradation of the DOPO group in Lig-K-DOPO produces phosphoric acid derivatives, which can be further transformed into polyphosphoric acid derivatives by dehydration of the P−OH bond.[42] These P-based acid derivatives could react with the OH groups in undecomposed/decomposed lignin and EG by esterification and dehydration, thus promoting the formation of intumescent P-rich char layers with polyaromatic structures bridged by P−O−C and P−O−P bonds. The char layer could be an effective thermal insulating layer to slow down the heat and mass transfer between the flame zone and the burning matrix. In addition, the Si−O−C bond in Lig-K-DOPO could inhibit the pyrolysis of SBR chains, generating a Si−O−C/Si−O−Si thermal insulation layer to reinforce the char layer. The nano-silica produced by the degradation of the Si−O−C/Si−O−Si bond could also migrate to the char surface during combustion, improving the integrity and quality of the char layer.[43] Consequently, the flame retardancy of Lig-K-DOPO-filled SBR samples was enhanced.

4. CONCLUSIONS

Based on the Atherton−Todd reaction and the hydrolysis/condensation reaction, the triple Si, P, and N-grafted lignin-based flame-retardant (Lig-K-DOPO) was synthesized using the flame-retardant intermediate DOPO with lignin via the linkage of silane coupling agent KH550. The results showed that the thermal stability of Lig-K-DOPO was much higher than that of lignin, increasing the curing rate and crosslinking density of the silica-filled SBR compounds. Associated with the improved filler dispersion of Lig-K-DOPO in the SBR matrix, the SBR/Lig-K-DOPO composites exhibited enhanced physical and mechanical properties compared to the SBR/lignin composites. Furthermore, Lig-K-DOPO showed good synergistic flame retardancy with EG and HPCTP. As Lig-K-DOPO increased, the HRR and SPR of the SBR vulcanizates decreased, and the time corresponding to the peak HRR was significantly prolonged, indicating the excellent flame retardancy of Lig-K-DOPO.

AUTHOR INFORMATION

Corresponding Authors

Shengqin Zhao − *Chair of Composite Engineering (CCe), Technische Universität Kaiserslautern (TUK), Kaiserslautern 67663, Germany*; Email: shengqin.zhao@mv.uni-kl.de

He Wang − *Key Laboratory of Rubber-Plastics of Ministry of Education/Shandong Provincial Key Laboratory of Rubber-Plastics, School of Polymer Science and Engineering, Qingdao University of Science & Technology, Qingdao 266042, China*; orcid.org/0000-0003-2758-5857; Email: wanghepolymer@qust.edu.com

Authors

Jianxing Li − *Key Laboratory of Rubber-Plastics of Ministry of Education/Shandong Provincial Key Laboratory of Rubber-Plastics, School of Polymer Science and Engineering, Qingdao University of Science & Technology, Qingdao 266042, China*

Zepei Yan − *Key Laboratory of Rubber-Plastics of Ministry of Education/Shandong Provincial Key Laboratory of Rubber-Plastics, School of Polymer Science and Engineering, Qingdao University of Science & Technology, Qingdao 266042, China*

Ming Liu − *Key Laboratory of Rubber-Plastics of Ministry of Education/Shandong Provincial Key Laboratory of Rubber-Plastics, School of Polymer Science and Engineering, Qingdao University of Science & Technology, Qingdao 266042, China*

Xiaokun Han − *Key Laboratory of Rubber-Plastics of Ministry of Education/Shandong Provincial Key Laboratory of Rubber-Plastics, School of Polymer Science and Engineering, Qingdao University of Science & Technology, Qingdao 266042, China*

Tianyun Lu − *Key Laboratory of Rubber-Plastics of Ministry of Education/Shandong Provincial Key Laboratory of Rubber-Plastics, School of Polymer Science and Engineering, Qingdao University of Science & Technology, Qingdao 266042, China*

Ruiyin Liu − *Key Laboratory of Rubber-Plastics of Ministry of Education/Shandong Provincial Key Laboratory of Rubber-Plastics, School of Polymer Science and Engineering, Qingdao University of Science & Technology, Qingdao 266042, China*

https://doi.org/10.1021/acsomega.3c00714
ACS Omega 2023, 8, 21549−21558

Shugao Zhao − *Key Laboratory of Rubber-Plastics of Ministry of Education/Shandong Provincial Key Laboratory of Rubber-Plastics, School of Polymer Science and Engineering, Qingdao University of Science & Technology, Qingdao 266042, China*

Qing Lv − *Jiangyin Haida Rubber and Plastic Co., Ltd., Jiangyin 214424, China*

Bo Li − *Jiangyin Haida Rubber and Plastic Co., Ltd., Jiangyin 214424, China*

Complete contact information is available at: https://pubs.acs.org/10.1021/acsomega.3c00714

Author Contributions

J.L.: Methodology, investigation, and writing original draft. Z.Y. and M.L.: Part experiment and data processing. T.L. and X.H.: Data processing and analysis. R.L., S.Z., Q.L., and B.L.: Manuscript review. H.W. and S.Z.: Conceptualization, supervision, methodology, investigation, and writing review & editing.

Notes

The authors declare no competing financial interest.

■ ACKNOWLEDGMENTS

The authors gratefully acknowledge the Natural Science Foundation of Shandong Province (CN), Grant/Award Number: ZR2020QE073.

■ REFERENCES

(1) Mauerer, O. New reactive, New reactive, halogen-free flame retardant system for epoxy resins. *Polym. Degrad. Stab.* **2005**, *88*, 70−73.

(2) Lu, S. Y.; Hamerton, I. Recent developments in the chemistry of halogen-free flame retardant polymers. *Prog. Polym. Sci.* **2002**, *27*, 1661−1712.

(3) Nageswara Rao, T.; Naidu, T. M.; Kim, M. S.; Parvatamma, B.; Prashanthi, Y.; Heun Koo, B. Influence of Zinc Oxide Nanoparticles and Char Forming Agent Polymer on Flame Retardancy of Intumescent Flame Retardant Coatings. *Nanomaterials* **2020**, *10*, 42.

(4) Xu, B.; Liu, Y. T.; Wei, S. M.; Zhao, S. H.; Qian, L. J.; Chen, Y. J.; Shan, H.; Zhang, Q. L. A Phosphorous-Based Bi-Functional Flame Retardant Based on Phosphaphenanthrene and Aluminum Hypophosphite for an Epoxy Thermoset. *Int. J. Mol. Sci.* **2022**, *23*, 11256.

(5) Kong, Q.; Wu, T.; Zhang, H.; Zhang, Y.; Zhang, M.; Si, T.; Yang, L.; Zhang, J. Improving flame retardancy of IFR/PP composites through the synergistic effect of organic montmorillonite intercalation cobalt hydroxides modified by acidified chitosan[J]. *Applied Clay Science* **2017**, *146*, 230−237.

(6) Wang, Z. J.; Liu, Y. F.; Li, J. Regulating effects of nitrogenous bases on char structure and flame retardancy of polypropylene/intumescent flame retardant composites[J]. *ACS Sustainable Chem. Eng.* **2017**, *5* (3), 2375−2383.

(7) Yang, H. T.; Yu, B.; Xu, X. D.; Bourbigot, S.; Wang, H.; Song, P. A. Lignin-derived bio-based flame retardants toward high-performance sustainable polymeric materials. *Green Chem.* **2020**, *22*, 2129−2161.

(8) Hosoya, T.; Kawamoto, H.; Saka, S. Role of methoxyl group in char formation from lignin-related compounds. *J. Anal. Appl. Pyrolysis* **2009**, *84*, 79−83.

(9) Zhao, S. Q.; Li, J. X.; Yan, Z. P.; Lu, T. Y.; Liu, R. Y.; Han, X. K.; Cai, C. C.; Zhao, S. G.; Wang, H. Preparation of lignin-based filling antioxidant and its application in styrene-butadiene rubber. *J. Appl. Polym. Sci.* **2021**, *138*, 51281.

(10) Liang, D. X.; Zhu, X. J.; Dai, P.; Lu, X. Y.; Guo, H. Q.; Que, H.; Wang, D. D.; He, T.; Xu, C. Z.; Robin, H. M.; Luo, Z. Y.; Gu, X. L. Preparation of a novel lignin-based flame retardant for epoxy resin. *Mater. Chem. Phys.* **2021**, *259*, No. 124101.

(11) Li, B.; Zhang, X. C.; Su, R. Z. An investigation of thermal degradation and charring of larch lignin in the condensed phase: The effects of boric acid, guanyl urea phosphate, ammonium dihydrogen phosphate and ammonium polyphosphate. *Polym. Adv. Technol.* **2002**, *1*, 35−44.

(12) Ayoub, A.; Venditti, R. A.; Jameel, H.; Chang, H.-M. Effect of irradiation on the composition and thermal properties of softwood kraft lignin and styrene grafted lignin. *J. Appl. Polym. Sci.* **2014**, *131*, 39743.

(13) Dai, P.; Liang, M. K.; Ma, X. F.; Luo, Y. L.; He, M.; Gu, X. L.; Gu, Q.; Hussain, I.; Luo, Z. Y. Highly Efficient, Environmentally Friendly Lignin-Based Flame Retardant Used in Epoxy Resin. *ACS Omega* **2020**, *5*, 32084−32093.

(14) Wang, Y. L.; Zhang, Y. M.; Liu, B. Y.; Zhao, Q.; Qi, Y. X.; Wang, Y. M.; Sun, Z. Y.; Liu, B. J.; Zhang, N. N.; Hu, W.; Xie, H. M. A novel phosphorus-containing lignin-based flame retardant and its application in polyurethane. *Compos. Commun.* **2020**, *21*, No. 100382.

(15) Liu, L.; Qian, M.; Song, P.'a.; Huang, G.; Yu, Y.; Fu, S. Fabrication of Green Lignin-based Flame Retardants for Enhancing the Thermal and Fire Retardancy Properties of Polypropylene/Wood Composites[J]. *ACS Sustainable Chem. Eng.* **2016**, *4* (4), 2422−2431.

(16) Zhou, S.; Tao, R.; Dai, P.; Luo, Z. Y.; He, M. Two-step fabrication of lignin-based flame retardant for enhancing the thermal and fire retardancy properties of epoxy resin composites. *Polym. Compos.* **2020**, *41*, 2025−2035.

(17) Zhu, H. B.; Peng, Z. M.; Chen, Y. M.; Li, G. Y.; Wang, L.; Tang, Y.; Pang, R.; Khan, Z. U. H.; Wan, P. Y. Preparation and characterization of flame retardant polyurethane foams containing phosphorus−nitrogen-functionalized lignin. *RSC Adv.* **2014**, *4*, 55271−55279.

(18) Li, S.; Xie, W. Y.; Wilt, M.; Willoughby, J. A.; Rojas, O. J. Thermally Stable and Tough Coatings and Films Using Vinyl Silylated Lignin. *ACS Sustainable Chem. Eng.* **2018**, *6*, 1988−1998.

(19) Wang, S. B.; Wang, S. H.; Shen, M. G.; Xu, X.; Liu, H.; Wang, D.; Wang, H. X.; Shang, S. B. Biobased Phosphorus Siloxane-Containing Polyurethane Foam with Flame-Retardant and Smoke-Suppressant Performances. *ACS Sustainable Chem. Eng.* **2021**, *9*, 8623−8634.

(20) Buono, P.; Duval, A.; Verge, P.; Averous, L.; Habibi, Y. New Insights on the Chemical Modification of Lignin: Acetylation versus Silylation. *ACS Sustainable Chem. Eng.* **2016**, *4*, 5212−5222.

(21) Abdel-Hakim, A.; El-Basheer, T. M.; Abdelkhalik, A. Mechanical, acoustical and flammability properties of SBR and SBR-PU foam layered structure. *Polym. Test.* **2020**, *88*, No. 106536.

(22) Castrovinci, A.; Camino, G.; Drevelle, C.; Duquesne, S.; Magniez, C.; Vouters, M. Ammonium polyphosphate−aluminum trihydroxide antagonism in fire retarded butadiene−styrene block copolymer. *Eur. Polym. J.* **2005**, *41*, 2023−2033.

(23) Liu, Q. Q.; Song, L.; Lu, H. D.; Hu, Y.; Wang, Z. Z.; Zhou, S. Study on combustion property and synergistic effect of intumescent flame retardant styrene butadiene rubber with metallic oxides. *Polym. Adv. Technol.* **2009**, *20*, 1091−1095.

(24) Perera, I. E.; Litton, C. D. Quantification of Optical and Physical Properties of Combustion-Generated Carbonaceous Aerosols (<PM2.5)Using Analytical and Microscopic Techniques. *Fire Technol.* **2015**, *51*, 247−269.

(25) Deng, J. S.; Isayev, A. I. Injection molding of rubber compounds: experimentation and simulation. *Rubber Chem. Technol.* **1991**, *64*, 296−324.

(26) Herrera, R.; Erdocia, X.; Llano-Ponte, R.; Labidi, J. Characterization of hydrothermally treated wood in relation to changes on its chemical composition and physical properties. *J. Anal. Appl. Pyrol.* **2014**, *107*, 256−266.

(27) Suksabye, P.; Thiravetyan, P. Cr(VI) adsorption from electroplating plating wastewater by chemically modified coir pith. *J. Environ. Manage.* **2012**, *102*, 1−8.

(28) Vasiljević, J.; Jerman, I.; Jakša, G.; Alongi, J.; Malucelli, G.; Zorko, M.; Tomšič, B.; Simončič, B. Functionalization of cellulose fibres with DOPO-polysilsesquioxane flame retardant nanocoating. *Cellulose* **2015**, *22*, 1893−1910.
(29) Zhang, Y.; Yu, B.; Wang, B.; Liew, K. M.; Song, L.; Wang, C. M.; Hu, Y. Highly Effective P−P Synergy of a Novel DOPO-Based Flame Retardant for Epoxy Resin. *Ind. Eng. Chem. Res.* **2017**, *56*, 1245−1255.
(30) Yang, B.; Wei, Y.; Qiu, Y. P.; Ramakrishna, S.; Liu, Y. B. A novel bio-based, flame retardant and latent imidazole compound—Its synthesis and uses as curing agent for epoxy resins. *J. Appl. Polym. Sci.* **2022**, *139*, No. e53079.
(31) Ferry, L.; Dorez, G.; Taguet, A.; Otazaghine, B.; Lopez-Cuesta, J. M. Chemical modification of lignin by phosphorus molecules to improve the fire behavior of polybutylene succinate. *Polym. Degrad. Stab.* **2015**, *113*, 135−143.
(32) Zhang, Y. M.; Zhao, Q.; Li, L. Q.; Yan, R.; Zhang, J.; Duan, J. C.; Liu, B. J.; Sun, Z. Y.; Zhang, M. Y.; Hu, W.; Zhang, N. N. Synthesis of a lignin-based phosphorus-containing flame retardant and its application in polyurethane. *RSC Adv.* **2018**, *8*, 32252−32261.
(33) Brebu, M.; Vasile, C. Thermal degradation of lignin − a review. *Cellul. Chem. Technol.* **2010**, *44*, 353−363.
(34) Wang, S. R.; Ru, B.; Lin, H. Z.; Sun, W. X.; Luo, Z. Y. Pyrolysis behaviors of four lignin polymers isolated from the same pine wood. *Bioresour. Technol.* **2015**, *182*, 120−127.
(35) Liu, Q.; Wang, S. R.; Zheng, Y.; Luo, Z. Y.; Cen, K. F. Mechanism study of wood lignin pyrolysis by using TG−FTIR analysis. *J. Anal. Appl. Pyrol.* **2008**, *82*, 170−177.
(36) Cao, J.; Xiao, G.; Xu, X.; Shen, D. K.; Jin, B. S. Study on carbonization of lignin by TG-FTIR and high-temperature carbonization reactor. *Fuel Process. Technol.* **2013**, *106*, 41−47.
(37) Ismail, H.; Ishiaku, U. S.; Arinab, A. R.; Mohd Ishak, Z. A. The Effect of Rice Husk Ash as a Filler for Epoxidized Natural Rubber Compounds. *Int. J. Polym. Mater.* **1997**, *36*, 39−51.
(38) Bahl, K.; Swanson, N.; Pugh, C.; Jana, S. C. Polybutadiene-g-polypentafluorostyrene as a coupling agent for lignin-filled rubber compounds. *Polymer* **2014**, *55*, 6754−6763.
(39) Li, T.; Li, S.; Ma, T. J.; Zhong, Y.; Zhang, L. P.; Xu, H.; Wang, B. J.; Feng, X. L.; Sui, X. F.; Chen, Z. Z.; Mao, Z. P. Novel organic-inorganic hybrid polyphosphazene modified manganese hypophosphite shuttles towards the fire retardance and anti-dripping of PET. *Eur. Polym. J.* **2019**, *120*, No. 109270.
(40) Li, J.; Mo, X. H.; Li, Y.; Zou, H. W.; Liang, M.; Chen, Y. Influence of expandable graphite particle size on the synergy flame retardant property between expandable graphite and ammonium polyphosphate in semi-rigid polyurethane foam. *Polym. Bull.* **2018**, *75*, 5287−5304.
(41) Liu, D.; Ji, P.; Zhang, T.; Lv, J.; Cui, Y. A bi-DOPO type of flame retardancy epoxy prepolymer: Synthesis, properties and flame-retardant mechanism. *Polym. Degrad. Stab.* **2021**, *190*, 109629−109639.
(42) Wang, P.; Chen, L.; Xiao, H. Flame retardant effect and mechanism of a novel DOPO based tetrazole derivative on epoxy resin. *J. Anal. Appl. Pyrol.* **2019**, *139*, 104−113.
(43) Cao, X. W.; Zhao, W. J.; Huang, J. S.; He, Y.; Liang, X. G.; Su, Y. J.; Wu, W.; Li, R. K. Y. Interface engineering of graphene oxide containing phosphorus/nitrogen towards fire safety enhancement for thermoplastic polyurethane. *Compos. Commun.* **2021**, *27*, No. 100821.

https://doi.org/10.1021/acsomega.3c00714
ACS Omega 2023, 8, 21549−21558